

Coulomb Blockade in Angstrom-scale latent ion track channels

Yanbo Xie,^{1*,2} Deli Shi,² Wenhui Wang² and Ziheng Wang²

¹School of Aeronautics and Institute of Extreme Mechanics, Northwestern Polytechnical University

²School of Physical Science and Technology, Northwestern Polytechnical University

Xi'an, 710072, China

(Dated: November 18, 2022)

When channels were scaled down to the size of hydrated ions, ionic Coulomb blockade was discovered. However, the experimental CB phenomenon was rarely reported since Feng et.al., discovered in MoS_2 nanopore. By using latent-track membranes with diameter of 0.6 nm, we found the channels are nearly non-conductive in small voltage due to the blockade of cations bound at surface, however turns to be conductive as rising of voltage due to releasing of bound ions, which differs from the mechanisms in MoS_2 nanopore. By Kramers' escape framework, we rationalized an analytical equation to fit experimental results, uncovering new fundamental insights of ion transport in the smallest channels.

Introduction– Ionic transport in an angstrom scale channel is critical to understand and mimic the physiological mechanism of biology ion channels[1–3]. The developing of nanotechnology and materials enable to create angstrom-scale structures to study ion transport in such confinement, which has led to several peculiar discoveries[2, 4–6] and excellent separation capabilities[7–9]. The Coulomb Blockade (CB) is a unique phenomenon discovered in angstrom-scale channels [8, 10], which originated from solid nanoelectronics devices that electrons must overcome an energy barrier to transport through an island of electrons[11, 12]. The ionic CB in nanofluidics were proposed by M. Di Ventra et al., in MD simulation[13], which was considered as one of the possible reasons of ion selectivity in biology ion channels[14–16]. Feng et.al discovered a non-linear conduction by using nanopores on a single layer MoS_2 , attributed to the joint action of ion-dehydration and self-energy barrier as the ionic CB effects[8]. Although theories progressed rapidly including mechanisms of dehydration [9, 17], self-energy[8, 18, 19], Wien-effects[6, 20, 21], in addition more types of angstrom-scale pores/materials were used in the study of ionic transport[22–25], the CB effects in experiments were never reported in artificial channels since it was discovered in MoS_2 nanopore[15].

In this work, we fabricated the latent ion track channels with a simplified procedure according to the previous work [26, 27]. We characterized the channels with a most probable diameter of 0.60nm by isotherm adsorption of CO_2 gas molecules using Brunauer-Emmett-Teller (BET) model [28, 29], quantitatively approving the angstrom-scale latent track channels which were indeed a challenge.

We found a transition of high resistance (HR) to low resistance (LR) of the membranes as rising of an external electrical field in diluted salt solutions. Although the non-linear conduction in latent track channels appeared in the previous work[26, 30, 31], the mechanisms and analysis of the results were still far from clear. We found the power law of conductance at HR stage matched well with the conductivity of bulk solution, implying the conduction at low voltage is independent of the surface

charge density. Besides, the conduction at HR state suggests only effectively $\sim 0.1\%$ of channels were conductive by radius of 0.3nm. We suspect it was caused by the counterions bound to the surface charge, which blockades the transport of free ions (scheme shown in Fig 1a), approval by our MD simulation and well explained the mechanisms of conductance transition. Our CB mechanism differs from the CB effects discovered in single layer MoS_2 caused by self-energy barrier and dehydration of ions [8].

Using Kramer's escape framework, we rationalized with an analytical equation of the current to fit our experimental results. The fitted values uncovers insightful details of the ionic transport in angstrom scale channels, such as decreases of conductivity at concentrated solution, and reduction of energy barrier as rising of ion density and surface charge density in the channel, resulting a decrease of threshold voltage transiting to conductive state. Our results matched well with the Coulomb Blockade effects predicted by Kavokine [20], at a dielectric surface of "infinite" long angstrom-scale channels. Our experimental results and theoretical analysis possibly give insights of the ion transport in well-defined 1D angstrom-scale channel, useful for fundamental studies of ionic transport or practical applications in angstrom scale channels.

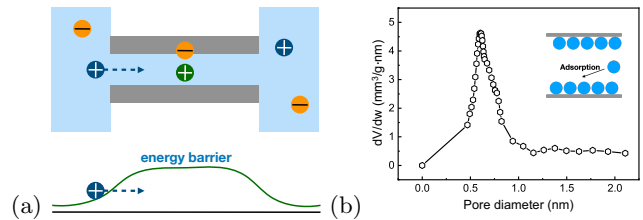


Figure 1. (a). The schematic picture of CB effect. A cation strongly bound to the surface charge, blockade the ion transport through the angstrom-scale channel. (b). The diameter distribution of latent track channels, characterized by the isotherm adsorption of CO_2 gas molecules. Our results showed the most probable diameter of latent track channels was 0.60nm.

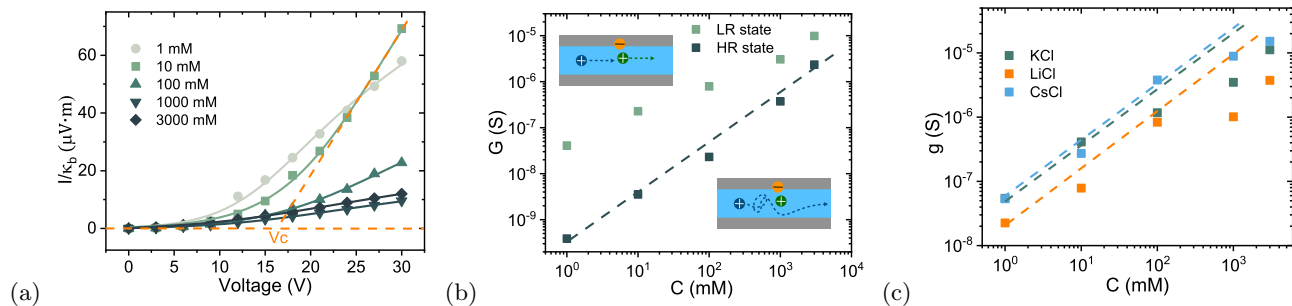


Figure 2. the typical I-V curves at positive applied potential in various concentrations. (b) The conductance of the HR (deep green) and LR (light green) as a function of concentration respectively. The possible mechanism of ionic transport were schematically drawn as inset figures. (c) the fitted conduction of Li^+ , K^+ , Cs^+ agreed well with the slope of κ_b when $C < 0.1M$, while apparently decreased when $C > 1M$.

Fabrications and Experimental setup– We first irradiated the polymer film by Kr ion with energy of over 1 MeV/u and density of $3 \times 10^8 cm^{-2}$ to form latent tracks in PET polymer films, from Lanzhou Heavy Ion Research Facility (HIRFL). Then we placed specimens under UV (365 nm) exposure with the illumination density of $65 mW \cdot cm^{-2}$ for over 30 minutes at each side. Finally, we clamped the irradiated polymer film in the 1mM KCl electrolyte solution bath in 50 degrees under voltage scanning ($\pm 10V$), to remove the products of radiolysis in the latent tracks thus fabricating one-dimensional ultrafine channels. The voltage scanning lasts for about half an hour until the amplitude of current get saturated shown as Fig.S1b. The film will be carefully cleaned by filling DI water under sweeping voltage, to remove the residual salts in the channels. The films were well preserved and dried in the air for overnight. For each experimental measurement, we keep the similar cleaning procedure above.

Precisely characterizing the size of the latent track channels is indeed a challenge. Traditional methods, including resistance measurements in 1M KCl, are inapplicable because it does not obey the classical conduction laws, as we demonstrated later. Hereby we use isotherms adsorption of CO_2 gas to characterize the size of channel, with details as follows.

To maximize surface area on the film, we irradiated the PET film with density of $10^{11} cm^{-2}$ ($6 \mu m$ thick) finally obtained $2.9 m^2/g$ BET surface area measured by Micromeritics 3Flex. We placed specimens in a vacuum chamber and gradually pressurized with CO_2 gas as rising of pressure of P/P_0 where P_0 is the atmosphere pressure. We measured the volume of absorbent in each applied pressure by recording the volume change of CO_2 over 15 seconds as a time step of equilibrium (see SM). As a result, we could linearly fit the adsorption kinetics according to Langmuir equation and calculate the surface area of the film. Finally, we calculated the diameter of channel distributed from 0.46 to 1.0 nm with a most probable diameter of 0.60 nm, where the smaller size were not detectable as the CO_2 molecules may not forming uniform Langmuir adsorption in such small channels

(Fig 1b). However, the factors during irradiation energy [32, 33], UV exposure [34], procedure of removing radiolysis products [27, 35] on the channel size are still not clear, even not the applications [36].

Results and Discussion– We first investigated the conductance as a function of the salt concentration C , ranging from 1 mM to 3M KCl at pH 5.0. To well present the current response in various concentrations, we showed the current divided by bulk conductivity of solution I/κ_b instead of current I in Fig 2a. We found non-linear I-V curves in low C . It appears a high resistance (HR) state at amplitude of voltage smaller than $\sim 3V$ for both polarity of electrical fields (See SM). Here we only demonstrated the results in positive bias voltages as examples for the analysis.

For the HR state, we linear fits the I-V curves at voltage smaller than 3V to obtain the conductance G_{HR} (dark green dots in Figure 2b), and calculated $G_{LR} = I_{+30V}/V_{+30V}$ as the conductance of LR state (light green dots in Figure 2 b). We found the G_{HR} perfectly matched with the power-law of κ_b (dashed lines) without a plateau in low concentrations as classical nanofluidics[37], which possibly implies the conduction is independent of surface charges under such low voltage. We calculated the numbers of conductive channels by G_{HR} using classical nanofluidic conduction theories which shows only $\sim 0.1\%$ channels are conductive using diameter of 0.60nm. To validate the electrical field dependent conduction, we investigated conduction using thicknesses of $2.5 \mu m$, $6 \mu m$, and $12 \mu m$. The results show that the threshold voltage for conductance transition decreases with the film thickness, but remains nearly a constant at $\sim 1V/\mu m$. The results are available in SM.

Above clues from experiments inspired us that the HR states of our results were possibly caused by the ionic Coulomb blockade. We performed MD simulations in the CNT with effective diameter of $0.55 nm$ comparable to the diameter measured by isotherm adsorption (see SM). We set a single carbon atom at surface been fully charged by an elementary charge of e , to mimic the dissociation of carboxyl groups at dielectric surface. Similar as previous work [6, 38, 39], we found strong Coulomb interaction be-

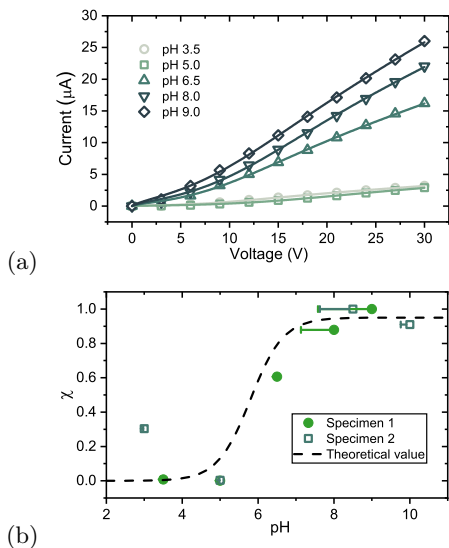


Figure 3. (a) the typical I-V curves in 10 mM KCl solution with pH from 3.5 to 9.5. (b) the fitted conductance from the individual experiments, matched well with the chemical equilibrium in different pH values.

tween the surface charge and counterions, resulting the blockade of ionic transport through the angstrom-scale channel. The small electrical field is not able to “excite” the bound ion, while the conduction relies on the free ions passing by the bound ions. As the electrical field increases, the probability of releasing the bound ions increases, resulting an “open” state for ion transport as a LR state.

Besides the Coulomb interaction between cation and surface charge, additional energy barrier including dehydration [9, 40], self-energy [18], and Bjerrum ion pairs [6] may play a role. For an approximation, we considered an equivalent parabolic potential barrier with a height of potential barrier ΔU , which may from one or joint actions of above effects. Thus, we have an analytical expression for the 1D ionic transport by Kramer’s escape approximation. The detailed derivation of current can be found in the SM. Thus, we have the following form of equations that used for fitting I-V curves, slightly different from the Hodgkin-Huxley model [41].

$$I = \frac{gV}{1 + kVe^{-bV}} \quad (1)$$

where the g, k and b are the fitted parameters, and V is the applied voltage. The fitting parameter $g = N \cdot \mu C A_{ch} / L$ are the conduction of all channels with number of N , considering free ions from the bulk solution with concentration of C_b and bound ions C_s at surface $C = C_b + C_s$. The A_{ch} is the mean cross-sectional area of a single channel. When energy barrier is negligible, the equation 1 turns to the classical nanofluidic conduction that linear increases as the applied voltage [42]. For the energy barrier dominated ion transport, it

becomes the same formula as Arrhenius type behavior in biology ion channels [43] and angstrom-scale slits [7, 44]. The entrance effects was neglected as we have “infinite” long channels ($r \ll L$) [45, 46]. Besides, we only considered the transport of metal ions as we found the Cl^- were not involved in the conduction in negatively charged angstrom channels in MD simulation. The fitting parameter $k \sim \mu e^{\Delta U / k_B T}$ where the ΔU is the energy barrier for ion transport through the confined channel. The fitting parameter b indicates the strength of electrical force on the bound ions, which is a constant between 0.20 to 0.25 V^{-1} for each specimen as in different concentrations (See SM), however slightly rises to maximal 0.4 V^{-1} as pH increases. The deviation of b in different specimens is possibly relevant to fabrication procedures such as radiolysis of films, which still need to be studied in further.

The fitted conduction g was shown as solid dots in Fig 2c as a function of C_b with different monovalent salt solution. The dashed lines represent the slope of κ_b in various salt solutions. The power law of experimental conduction (solid dots) matched well with κ_b below 0.1M, however obviously getting smaller than κ_b above 1M. We suspect this reduction of conductivity was caused by the formation of ion pairs in the angstrom scale channel, previously reported in the slits nanochannels [6, 47] and CNT [6, 48–50]. Since only free ions contribute to the conduction in small HR state, we suspect the formation of ion pairs as increases of C_b results the reduction of conductivity[51].

Then we studied the conduction under various pH solutions (Fig.3a). Our results showed the amplitude of conduction gradually increases as the pH values. In addition, the system gets close to Ohmic as the pH rises. The fitted conduction g including the bound ions in the channel gradually increases and then get saturated as the pH values, shown in the Fig. 3b. According to the chemical equilibrium at surface that the surface charge density varies as the pH using following equations [52].

$$\Sigma = -e\Gamma \frac{10^{-pK}}{10^{-pK} + 10^{-pH}} \quad (2)$$

where e is the elementary charge. We obtained the site density Γ of carboxyl groups at the surface as $\sim 10^{-2} \text{site/nm}^2$ that is smaller than that in the track etched nanopores [53], possibly due to the lacking of chemical etching. We obtained dissociation factor as $\chi = 10^{-pK} / (10^{-pK} + 10^{-pH})$, where the pK was taken as 5.8 for the carboxyl group [52]. Taking the counterions in the conductance $g_\Sigma = N \cdot \mu C_\Sigma A_{ch} / L$ where $C_\Sigma = \frac{2\Gamma}{rN_A}$ and N_A is Avogadro number, we have a theoretical value shown as solid line in Fig. 3 b. The buffer solutions were avoided due to their profound effects for chemical equilibrium at surface [54]. The error bars indicate the pH change during the measurements (~ 20 mins), caused by the adsorption of CO_2 from air. The deviation of experimental data at pH=3.0 possible caused by the inversion of surface charge, which doesn’t fits the theoretical prediction in equation 2.

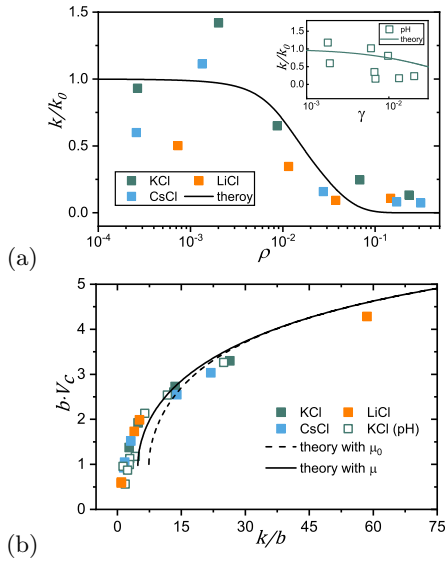


Figure 4. (a) The fitted parameter k/k_0 decreases as ρ and γ (inset) matching well with the theoretical predictions (solid line). (b) the critical voltage increases as k/μ , matching well with the experiments calculated with constant ion mobility (dashed line) and in mobility decreases in high concentrations (solid line).

Now we focused another fitting parameter k . The linear density of free ions can be calculated as $d_f = (A_{ch}N_A C_b)^{-1}$, while the linear density of bound ion density as $d_s = (A_{ch}N_A \frac{2}{r} \Sigma)^{-1}$. We have the linear ion density $\rho = x_T/d_f$, where $x_T = a^2/(2l_B)$ is thermal length of an ion. The potential barrier U rapidly decreases as the entropy of the channel increases due to the dissociation of bound ion or ion pairs predicted by Zhang as follows [55, 56].

$$U = U_0 [1 - 4\gamma \ln(\frac{1}{2\rho} \sinh(\frac{\rho}{\gamma}))] \quad (3)$$

Finally, we evaluated the $k/k_0 \sim \mu e^{(U-U_0)/k_B T}$ as a function of ion density ρ and surface charge density γ shown as a solid line in Fig.4a, considering the reduction of mobility compared to the bulk values. The increases of ion density, including the concentration of free ions and bound ions at surface, reducing the energy barrier of transport. As a result, current getting close to the linear response to the applied voltage. We statistically counted all fitted k/k_0 as a function of ρ derived from C_b shown in 4a, and $\gamma = x_T \cdot 2\pi r \Gamma \chi$ derived from the equation 2 as an inset figure in 4a. The theoretical k/k_0 by equation 3 matched well with the fitted values in experiments.

To quantitatively evaluate the critical voltage of conduction states transition, we linear fits the I-V curves at LR states and considered a crossing point to the X-axis as V_C , with an example shown as a dashed line in the I-V curves in Fig.2a. Details of deriving the critical voltage in experiments can be found in the SM. From the theoretical aspects, we estimate the transition voltage V_C by $kV e^{-bV_C} = e$, where the current starts rising apparently. Thus we have the solution as follows, where the $W(z)$ is Lambert W Function.

$$V_C = -W(-\frac{e \cdot b}{k})/b \quad (4)$$

With all fitted k and b from experiments, we showed the V_C considering different types of salts, concentrations and pH values of the film in the Fig. 4b. The theoretical values by equation 4 considering the free ion density ρ and surface charge density γ , well predicting the tendency of V_C in experiments that is helpful for understanding 1D ionic transport due to CB effects.

Conclusion– In conclusion, we fabricated latent ion-track channels and characterized 0.60nm as most probable diameter by the isotherm gas adsorptions. We found a resistance transition from HR to LR state as rises of applied voltage in diluted solutions. We suspect the HR state was caused by the counterions bound to the surface charge that blockades the ion transport due to the strong Coulomb interaction to the surface charge in confinements, approved by MD simulations. The conduction at HR state matched well with the slope of bulk conductivity, illustrating the counterions didn't contribute to the conduction. As increases of E , the probability of releasing bound ions increases, resulting LR state. We rationalized an analytical equation by Kramer's escaping approximation, with an equivalent parabolic potential barrier for ion transport, uncovering more insights of ion transport, such as the reduction of conductivity in channels at concentrated salt solutions and decrease of energy barrier as increases of ions density. Our results will be useful for the fundamental studies of ion transport in the smallest scale channels, as well as the application aspects like separations.

ACKNOWLEDGMENTS

The authors thank Jinglai Duan, Jie Liu and Guanghua Du in HIRFL for the help of film irradiation, Shusong Zhang for useful discussions, Xianzhi Ke and Shenghui Guo for the experimental help, Jianwei Cao and Kaijie Chen for the help of isotherm adsorption. This work is supported by NSFC No. 12075191.

[1] S. Faucher, N. Aluru, M. Z. Bazant, D. Blankschtein, A. H. Brozena, J. Cumings, J. Pedro de Souza, M. Elim-

elech, R. Epsztein, J. T. Fourkas, A. G. Rajan, H. J. Kulik, A. Levy, A. Majumdar, C. Martin, M. McEL-

- drew, R. P. Misra, A. Noy, T. A. Pham, M. Reed, E. Schwegler, Z. Siwy, Y. Wang, and M. Strano, Critical Knowledge Gaps in Mass Transport through Single-Digit Nanopores: A Review and Perspective, *The Journal of Physical Chemistry C* **123**, 21309 (2019).
- [2] L. Bocquet, Nanofluidics coming of age, *Nature Materials* **19**, 254 (2020).
- [3] P. Robin, N. Kavokine, and L. Bocquet, Modeling of emergent memory and voltage spiking in ionic transport through angstrom-scale slits, *Science* **373**, 687 (2021).
- [4] B. Radha, A. Esfandiar, F. C. Wang, A. P. Rooney, K. Gopinadhan, A. Keerthi, A. Mishchenko, A. Janardanan, P. Blake, L. Fumagalli, M. Lozada-Hidalgo, S. Garaj, S. J. Haigh, I. V. Grigorieva, H. A. Wu, and A. K. Geim, Molecular transport through capillaries made with atomic-scale precision, *Nature* **538**, 222 (2016).
- [5] L. Fumagalli, A. Esfandiar, R. Fabregas, S. Hu, P. Ares, A. Janardanan, Q. Yang, B. Radha, T. Taniguchi, K. Watanabe, G. Gomila, K. S. Novoselov, and A. K. Geim, Anomalously low dielectric constant of confined water, *Science* **360**, 1339 (2018).
- [6] N. Kavokine, S. Marbach, A. Siria, and L. Bocquet, Ionic coulomb blockade as a fractional wien effect, *Nature Nanotechnology* **14**, 573 (2019).
- [7] P. Z. Sun, M. Yagmurcukardes, R. Zhang, W. J. Kuang, M. Lozada-Hidalgo, B. L. Liu, H.-M. Cheng, F. C. Wang, F. M. Peeters, I. V. Grigorieva, and A. K. Geim, Exponentially selective molecular sieving through angstrom pores, *Nature Communications* **12**, 7170 (2021).
- [8] J. Feng, M. Graf, K. Liu, D. Ovchinnikov, D. Dumcenco, M. Heiranian, V. Nandigana, N. R. Aluru, A. Kis, and A. Radenovic, Single-layer MoS₂ nanopores as nanopower generators, *Nature* **536**, 197 (2016).
- [9] Y. Fu, S. Su, N. Zhang, Y. Wang, X. Guo, and J. Xue, Dehydration-Determined Ion Selectivity of Graphene Subnanopores, *ACS Applied Materials & Interfaces* **12**, 24281 (2020).
- [10] N. Kavokine, R. R. Netz, and L. Bocquet, Fluids at the Nanoscale: From Continuum to Subcontinuum Transport, *Annual Review of Fluid Mechanics* **53**, 377 (2021).
- [11] T. A. Fulton and G. J. Dolan, Observation of single-electron charging effects in small tunnel junctions, *Physical Review Letters* **59**, 109 (1987).
- [12] L. Clarke, M. N. Wybourne, M. Yan, S. X. Cai, and J. F. W. Keana, Transport in gold cluster structures defined by electron-beam lithography, *Applied Physics Letters* **71**, 617 (1997).
- [13] M. Krems and M. Di Ventra, Ionic Coulomb blockade in nanopores, *Journal of Physics: Condensed Matter* **25**, 065101 (2013).
- [14] I. K. Kaufman, P. V. E. McClintock, and R. S. Eisenberg, Coulomb blockade model of permeation and selectivity in biological ion channels, *New Journal of Physics* **17**, 083021 (2015).
- [15] A. Chernev, S. Marion, and A. Radenovic, Prospects of Observing Ionic Coulomb Blockade in Artificial Ion Confinements, *Entropy* **22**, 1430 (2020).
- [16] I. Kaufman, D. G. Luchinsky, R. Tindjong, P. V. E. McClintock, and R. S. Eisenberg, Multi-ion conduction bands in a simple model of calcium ion channels, *Physical Biology* **10**, 026007 (2013).
- [17] M. L. Barabash, W. A. T. Gibby, C. Guardiani, A. Smolyanitsky, D. G. Luchinsky, and P. V. E. McClintock, Origin and control of ionic hydration patterns in nanopores, *Communications Materials* **2**, 65 (2021).
- [18] A. Parsegian, Energy of an Ion crossing a Low Dielectric Membrane: Solutions to Four Relevant Electrostatic Problems, *Nature* **221**, 844 (1969).
- [19] S. Teber, Translocation energy of ions in nano-channels of cell membranes, *Journal of Statistical Mechanics: Theory and Experiment* **2005**, P07001 (2005).
- [20] N. Kavokine, P. Robin, and L. Bocquet, Interaction confinement and electronic screening in two-dimensional nanofluidic channels, *The Journal of Chemical Physics* **157**, 114703 (2022).
- [21] B. Coquinot, L. Bocquet, and N. Kavokine, Quantum feedback at the solid-liquid interface: flow-induced electronic current and negative friction (2022), arXiv:2205.03250 [cond-mat].
- [22] C. Cheng, S. A. Iyengar, and R. Karnik, Molecular size-dependent subcontinuum solvent permeation and ultrafast nanofiltration across nanoporous graphene membranes, *Nature Nanotechnology* 10.1038/s41565-021-00933-0 (2021).
- [23] T. Jain, B. C. Rasera, R. J. S. Guerrero, M. S. H. Boutilier, S. C. O'Hern, J.-C. Idrobo, and R. Karnik, Heterogeneous sub-continuum ionic transport in statistically isolated graphene nanopores, *Nature Nanotechnology* **10**, 1053 (2015).
- [24] J. Lu, H. Xu, H. Yu, X. Hu, J. Xia, Y. Zhu, F. Wang, H.-A. Wu, L. Jiang, and H. Wang, Ultrafast rectifying counter-directional transport of proton and metal ions in metal-organic framework-based nanochannels, *Science Advances* **8**, eabl5070 (2022).
- [25] M. E. Suk and N. R. Aluru, Ion transport in sub-5-nm graphene nanopores, *The Journal of Chemical Physics* **140**, 084707 (2014).
- [26] Q. Wen, D. Yan, F. Liu, M. Wang, Y. Ling, P. Wang, P. Kluth, D. Schauries, C. Trautmann, P. Apel, W. Guo, G. Xiao, J. Liu, J. Xue, and Y. Wang, Highly Selective Ionic Transport through Subnanometer Pores in Polymer Films, *Advanced Functional Materials* **26**, 5796 (2016).
- [27] P. Wang, M. Wang, F. Liu, S. Ding, X. Wang, G. Du, J. Liu, P. Apel, P. Kluth, C. Trautmann, and Y. Wang, Ultrafast ion sieving using nanoporous polymeric membranes, *Nature Communications* **9**, 569 (2018).
- [28] S. Brunauer, P. H. Emmett, and E. Teller, Adsorption of Gases in Multimolecular Layers, *Journal of the American Chemical Society* **60**, 309 (1938).
- [29] K.-J. Chen, D. G. Madden, S. Mukherjee, T. Pham, K. A. Forrest, A. Kumar, B. Space, J. Kong, Q.-Y. Zhang, and M. J. Zaworotko, Synergistic sorbent separation for one-step ethylene purification from a four-component mixture, *Science* **366**, 241 (2019).
- [30] S. Wu, Y. Cheng, J. Ma, Q. Huang, Y. Dong, J. Duan, D. Mo, Y. Sun, J. Liu, and H. Yao, Preparation and ion separation properties of sub-nanoporous PES membrane with high chemical resistance, *Journal of Membrane Science* **635**, 119467 (2021).
- [31] Y. Cheng, Y. Dong, Q. Huang, K. Huang, S. Lyu, Y. Chen, J. Duan, D. Mo, Y. Sun, J. Liu, Y. Peng, and H. Yao, Ionic Transport and Sieving Properties of Sub-nanoporous Polymer Membranes with Tunable Channel Size, *ACS Applied Materials & Interfaces* **13**, 9015 (2021).
- [32] X. Wang, S. Dutt, C. Notthoff, A. Kiy, P. Mota-Santiago, S. T. Mudie, M. E. Toimil-Molares, F. Liu, Y. Wang, and

- P. Kluth, SAXS data modelling for the characterisation of ion tracks in polymers, *Physical Chemistry Chemical Physics* **24**, 9345 (2022).
- [33] P. Y. Apel, I. Blonskaya, T. Cornelius, R. Neumann, R. Spohr, K. Schwartz, V. Skuratov, and C. Trautmann, Influence of temperature during irradiation on the structure of latent track in polycarbonate, *Radiation Measurements* **44**, 759 (2009).
- [34] Z. Zhu, Y. Maekawa, Q. Liu, and M. Yoshida, Influence of UV light illumination on latent track structure in PET, *Nuclear Instruments and Methods in Physics Research Section B: Beam Interactions with Materials and Atoms* **236**, 61 (2005).
- [35] P. Y. Apel, I. Blonskaya, O. Ivanov, O. Kristavchuk, A. Nechaev, K. Olejniczak, O. Orelovich, O. Polezhaeva, and S. Dmitriev, Do the soft-etched and UV-track membranes actually have uniform cylindrical subnanometer channels?, *Radiation Physics and Chemistry* **198**, 110266 (2022).
- [36] M. H. Ali Haider, S. Nasir, M. Ali, P. Ramirez, J. Cervera, S. Mafe, and W. Ensinger, Osmotic energy harvesting with soft-etched nanoporous polyimide membranes, *Materials Today Energy* **23**, 100909 (2022).
- [37] D. Stein, M. Kruithof, and C. Dekker, Surface-Charge-Governed Ion Transport in Nanofluidic Channels, *Physical Review Letters* **93**, 035901 (2004).
- [38] R. Qiao and N. R. Aluru, Atypical Dependence of Electroosmotic Transport on Surface Charge in a Single-wall Carbon Nanotube, *Nano Letters* **3**, 1013 (2003).
- [39] Y. Xie, L. Fu, T. Niehaus, and L. Joly, Liquid-Solid Slip on Charged Walls: The Dramatic Impact of Charge Distribution, *Physical Review Letters* **125**, 014501 (2020), number: 1.
- [40] S. Sahu, M. Di Ventra, and M. Zwolak, Dehydration as a Universal Mechanism for Ion Selectivity in Graphene and Other Atomically Thin Pores, *Nano Letters* **17**, 4719 (2017).
- [41] A. L. Hodgkin and A. F. Huxley, A quantitative description of membrane current and its application to conduction and excitation in nerve, *The Journal of Physiology* **117**, 500 (1952).
- [42] L. Bocquet and E. Charlaix, Nanofluidics, from bulk to interfaces, *Chem. Soc. Rev.* **39**, 1073 (2010).
- [43] A. Chernyshev and S. Cukierman, Thermodynamic View of Activation Energies of Proton Transfer in Various Gramicidin A Channels, *Biophysical Journal* **82**, 182 (2002).
- [44] S. Hu, K. Gopinadhan, A. Rakowski, M. Neek-Amal, T. Heine, I. V. Grigorieva, S. J. Haigh, F. M. Peeters, A. K. Geim, and M. Lozada-Hidalgo, Transport of hydrogen isotopes through interlayer spacing in van der Waals crystals, *Nature Nanotechnology* **13**, 468 (2018).
- [45] Y. Ma, J. Guo, L. Jia, and Y. Xie, Entrance Effects Induced Rectified Ionic Transport in a Nanopore/Channel, *ACS Sensors* **3**, 167 (2018).
- [46] M. Macha, S. Marion, V. V. R. Nandigana, and A. Radenovic, 2D materials as an emerging platform for nanopore-based power generation, *Nature Reviews Materials* **4**, 588 (2019).
- [47] W. Zhao, Y. Sun, W. Zhu, J. Jiang, X. Zhao, D. Lin, W. Xu, X. Duan, J. S. Francisco, and X. C. Zeng, Two-dimensional monolayer salt nanostructures can spontaneously aggregate rather than dissolve in dilute aqueous solutions, *Nature Communications* **12**, 5602 (2021).
- [48] D. Nicholson and N. Quirke, Ion Pairing in Confined Electrolytes, *Molecular Simulation* **29**, 287 (2003).
- [49] V. Neklyudov and V. Freger, Putting together the puzzle of ion transfer in single-digit carbon nanotubes: mean-field meets *ab initio*, *Nanoscale* **14**, 8677 (2022).
- [50] F. Aydin, A. Moradzadeh, C. L. Bilodeau, E. Y. Lau, E. Schwegler, N. R. Aluru, and T. A. Pham, Ion solvation and transport in narrow carbon nanotubes: Effects of polarizability, cation π interaction, and confinement, *Journal of Chemical Theory and Computation* **17**, 1596 (2021).
- [51] T. J. Yoon, L. A. Patel, M. J. Vigil, K. A. Maerzke, A. T. Findikoglu, and R. P. Currier, Electrical conductivity, ion pairing, and ion self-diffusion in aqueous NaCl solutions at elevated temperatures and pressures, *The Journal of Chemical Physics* **151**, 224504 (2019).
- [52] S. H. Behrens and D. G. Grier, The charge of glass and silica surfaces, *The Journal of Chemical Physics* **115**, 6716 (2001).
- [53] C.-Y. Lin, L.-H. Yeh, and Z. S. Siwy, Voltage-Induced Modulation of Ionic Concentrations and Ion Current Rectification in Mesopores with Highly Charged Pore Walls, *The Journal of Physical Chemistry Letters* **9**, 393 (2018).
- [54] M. Boström, D. R. M. Williams, and B. W. Ninham, Specific ion effects: Role of salt and buffer in protonation of cytochrome c, *The European Physical Journal E* **13**, 239 (2004).
- [55] J. Zhang, A. Kamenev, and B. I. Shklovskii, Conductance of Ion Channels and Nanopores with Charged Walls: A Toy Model, *Physical Review Letters* **95**, 148101 (2005).
- [56] J. Zhang, A. Kamenev, and B. I. Shklovskii, Ion exchange phase transitions in water-filled channels with charged walls, *Physical Review E* **73**, 051205 (2006).